Available online at www.sciencedirect.com

ScienceDirect

Journal of the European Ceramic Society 28 (2008) 139–147

www.elsevier.com/locate/jeurceramsoc

Processing of AB-type carbonated hydroxyapatite $Ca_{10-x}(PO_4)_{6-x}(CO_3)_x(OH)_{2-x-2y}(CO_3)_y$ ceramics with controlled composition

J.P. Lafon [a], E. Champion [a,*], D. Bernache-Assollant [b]

[a] SPCTS, Université de Limoges, CNRS, Faculté des Sciences et Techniques, 123 Avenue Albert Thomas, 87060 Limoges Cedex, France
[b] CIS, ENS des Mines, 158 cours Fauriel, 42023 Saint-Etienne Cedex 2, France

Received 24 September 2006; received in revised form 30 May 2007; accepted 9 June 2007
Available online 28 August 2007

Abstract

This work is devoted to the preparation of carbonated calcium phosphate apatites. The aim was to produce dense ceramics containing various and precisely controlled amounts of carbonate ions partially substituting either for phosphate (B-type apatites) or for hydroxide ions (A-type apatites). Powders were synthesized by a wet chemical process in aqueous media. Heating carbonated powders above 600 °C in air or neutral atmosphere led to their thermal decomposition. A CO_2 gas partial pressure of 50 kPa in the atmosphere stabilized the carbonated apatites up to temperatures allowing their sintering. But, CO_2 gas induced a carbonation of hydroxide sites (A-site) that was detrimental to the sintering. A low partial pressure of water vapour in the atmosphere proved to be efficient to control A-site carbonation and indirectly favoured the sintering. Dense ceramics made of single phased apatite $Ca_{10-x}(PO_4)_{6-x}(CO_3)_x(OH)_{2-x-2y}(CO_3)_y$, with $0 \le x \le 1.1$ and $0 \le y \le 0.2$ could be produced. The value of x (B-type carbonates) was controlled by the synthesis process and the value of y (A-type carbonates) by the sintering atmosphere.

Keywords: Powders-chemical preparation; Sintering; Apatite; Biomedical applications

1. Introduction

Due to a chemical composition close to that of the bone mineral, calcium phosphate hydroxyapatite, formula $Ca_{10}(PO_4)_6(OH)_2$-HA-, has proved to be an attractive material for biological applications.[1–4] It is commonly used as a synthetic bone substitute. The bony natural apatites contain carbonate ions in significant amount, from about 3 to 8 wt%, that partially substitute for both phosphate ions (PO_4^{3-}) in the B sites of the apatitic structure (B-type substitution), and hydroxide ions (OH^-) in the A sites (A-type substitution).[5–8]

Synthetic A-type carbonated apatites $Ca_{10}(PO_4)_6(OH)_{2-2y}(CO_3)_y$, with $0 \le y \le 1$, can be prepared by heating pure HA at 800–1000 °C for several hours in dry CO_2 atmosphere according to the following reaction:[9]

$$Ca_{10}(PO_4)_6(OH)_2 + yCO_2 \leftrightarrow Ca_{10}(PO_4)_6(OH)_{2-2y}(CO_3)_y + yH_2O \quad (1)$$

B-type carbonated apatite powders are generally synthesized from a precipitation reaction in aqueous media. Several parameters (pH, temperature, chemical nature of the reagents, reagent concentrations, etc.) control the chemical properties of the final powder.[10] Different chemical formulae are proposed in the literature to describe B-type carbonated apatites, the simplest and most commonly used is $Ca_{10-x}(PO_4)_{6-x}(CO_3)_x(OH)_{2-x}$, with $0 \le x \le 2$. But, because the apatite structure of the mineral bone contains sodium ions located in the calcium sites, B-type apatites are usually synthesized using sodium salts in order to mimic the natural structure. Sodium is also known to increase the maximum ratio of carbonate substitution in B-site because its incorporation in calcium sites induces a favourable electrical charge balance, which corresponds to the chemical formula $Ca_{10-x}Na_{2x/3}(PO_4)_{6-x}(CO_3)_x(OH)_{2-x/3}$, with $0 \le x \le 3$.[11]

---

[*] Corresponding author at: SPCTS, UMR CNRS 6638, Université de Limoges, 123 Avenue Albert Thomas, 87060 Limoges Cedex, France.
Tel.: +33 555457460; fax: +33 555457586.
E-mail address: eric.champion@unilim.fr (E. Champion).

0955-2219/$ – see front matter © 2007 Elsevier Ltd. All rights reserved.
doi:10.1016/j.jeurceramsoc.2007.06.009

According to studies carried out on sodium-containing carbonated hydroxyapatites (Na-CO_3-Aps), the introduction of carbonate ions in the HA would increase its dissolution rate in solution and could enhance its osteointegration rate.[12–14] But, as few studies have been devoted to the biological behaviour of pure single phased carbonated hydroxyapatites without alkali, the role of carbonate remains unclear. A high temperature thermal treatment is required to produce ceramic parts from powders. But, to obtain dense materials the sintering of carbonated apatites is often performed in a temperature range that induces carbonate losses, and thus, the partial or total decomposition of the material.[15–20] Though some attempts have been made to synthesize pure AB-type carbonated apatite powders[21] and ceramics,[22] the production of nearly fully dense ceramics (over 95% of the maximum density) with varying and controlled amounts of carbonate ions in A and B sites of the apatite structure has never been totally investigated and is still a difficulty.

Finally, because of the presence of secondary phases and/or of extra ions in the apatite structure as well as a poorly controlled carbonation ratio of sintered materials, the effect of location (A or B-type) and amount of carbonate ions on the biological behaviour of hydroxyapatite ceramics remains still unclear. In this aim, the processing of dense materials is necessary because the open porosity can be a significant microstructural parameter on the properties of materials (strength, solubility, etc.). This open porosity is well known to remain in ceramic materials up to a densification ratio of 92–95% of the maximum density. Denser materials exhibit only closed residual pores that do not modify the surface of the material or its properties.

On these bases, a study devoted to the processing of dense ceramics of single phased and sodium-free carbonated hydroxyapatites with controlled carbonate content was conducted to further evaluate the role of carbonate ions on the biological behaviour. The current paper is part of this study. It deals with the powder synthesis and the sintering of A/B type carbonated hydroxyapatite ceramics with controlled compositions.

2. Materials and methods

2.1. Powder synthesis

Powders were prepared by an aqueous precipitation method. Two hundred and fifty milliliters of an aqueous solution containing 0.24 mol of di-ammonium hydrogenphosphate ($(NH_4)_2HPO_4$, reagent grade, Aldrich, France) and from 0 to 2 mol of ammonium hydrogencarbonate ($(NH_4)HCO_3$, reagent grade, Aldrich, France) was added into a vessel containing 0.4 mol of calcium nitrate ($Ca(NO_3)_2 \cdot 4H_2O$, reagent grade, Aldrich, France) in 750 mL of distilled water. The synthesis device was a fully automated apparatus. The pH of the solution was maintained at the constant value of 9.0 (±0.1) by addition of a concentrated solution (28%) of ammonium hydroxide using a pH stat (Hanna Instrument). The temperature was controlled and regulated at 90 °C. The suspension was continuously stirred and refluxed. After total addition of the $(NH_4)_2HPO_4 + (NH_4)HCO_3$ solution, the suspension was ripened for 30 min. Then, it was filtered and washed with 200 mL of distilled water. The resulting precipitate was dried at 100 °C for at least 24 h. The raw powders, except HA, were heat treated for 2 h at 400 °C in air in order to eliminate the adsorbed moisture and the synthesis residues such as nitrous species. This thermal treatment did not modify the chemical composition of compounds.

Table 1
Sample notation and synthesis parameters

Sample	$(C/P)_{reagents}$	pH (±0.1)	Temperature (°C)
HA	0	8.0	95
C0125	1/8	9.0	90
C025	1/4	9.0	90
C05	1/2	9.0	90
C1	1	9.0	90
C2	2	9.0	90

The (Ca^{2+}/PO_4^{3-}) molar ratio of the initial reagents was maintained at the constant value of 10/6 for all the syntheses. Different values of the (CO_3^{2-}/PO_4^{3-}) molar ratio of the initial reagents ($(C/P)_{reagents}$) were chosen, from 0 to 2, in order to precipitate powders containing various amounts of CO_3^{2-}. The experimental parameters are summarized in Table 1. The vessel was placed in an argon atmosphere under dynamic flow to prevent any presence and dissolution of CO_2 from the ambient air in the reacting solutions, which could result in an uncontrolled (C/P) ratio and carbonation amount of the precipitates. The purity of the commercial reagents used in this study was systematically controlled.

2.2. Sintering

For sintering experiments and thermomechanical analyses (TMA-dilatometry) the powders were initially heat treated at 500 °C, i.e. below the decomposition temperature, for an adapted duration in order to reach the same surface area of about 30 $m^2 g^{-1}$ whatever the composition. Then, cylindrical samples were produced by uniaxial pressing of powders (0.4 g) followed by cold isostatic pressing under 200 MPa. The compaction ratio of samples before sintering was 60 ± 3% of the theoretical density.

Linear shrinkage was measured by dilatometry (Setaram, model TMA 92, France). Linear shrinkage is directly indicative of the sintering behaviour of the material providing no other phenomenon accompanied with volume changes that could mask sintering effects occurs simultaneously. The thermal cycle included a 10 min holding time at 1250 °C and the heating and cooling rate was 10 °C min^{-1}. The experiments were performed in an atmosphere of either CO_2 or argon flowing gas (10 L min^{-1}).

Sintering tests were carried out in controlled atmospheres of $Ar/CO_2/H_2O$ gaseous mixtures under flowing conditions in an alumina vertical furnace allowing a maximum temperature of 1400 °C. Argon was used as inert carrier gas and the total pressure was 100 kPa. Three atmospheres were tested: a dry atmosphere 50% Ar/50% CO_2 and two wet atmospheres 47% Ar/50% CO_2/3% H_2O or 35% Ar/50% CO_2/15% H_2O. The samples were placed in an open alumina crucible and rapidly brought

Table 2
Calculated values of maximum density (d_{th}) of samples before and after heat treatment in different atmospheres

Sample	Raw powder	50% Ar/50% CO_2	47% Ar–50% CO_2–3% H_2O	35% Ar–50% CO_2–15% H_2O
HA	3.156	n.d.[a]	n.d.	n.d.
C0125	3.04	3.06	3.05	3.05
C025	2.96	2.98	2.97	2.96
C05	2.90	2.91	2.90	2.90
C1	2.86	2.87	2.86	2.86

[a] n.d.: not determined.

from a cold area of the furnace into the preheated isothermal zone. This corresponded to a heating rate of about 100 °C min^{-1}. Samples were kept from 7 to 120 min at the sintering temperature that ranged from 825 to 950 °C. Then, they were rapidly cooled by the process opposite to that used for their heating.

2.3. Materials characterization

X-ray diffraction (XRD) patterns of powders and sintered ceramics were recorded with Cu Kα radiation on a $\theta/2\theta$ diffractometer (Siemens, Model D5000, Germany). The crystalline phases were determined from a comparison of the registered patterns with the ICDD powder diffraction files (PDF cards). The type of carbonate substitution (A, B or A/B-type) was identified in the powders and sintered pellets (after grinding) by infrared spectrometry on a Fourier transform spectrometer (Spectrum one, Perkin-Elmer, USA) with a resolution of 2 cm^{-1}. In order to allow comparisons, the spectra were normalized from the ν_4 band of the phosphate group at 602 cm^{-1} according to a classical procedure.[23]

The total weight content of carbonate ions in the powders and pellets was measured by elemental analysis (Elemental Analyser Model 1106, Carlo Erba Strumentazione, Italy).

Specific surface area (S_{BET}) and density (d) of powders were determined by the BET method (8 points, Analyser Micromeritics ASAP 2010, USA) and pycnometry analysis (Analyser Micromeritics AccuPyc 1330, USA), respectively. The average grain size (D) was estimated from the values of surface area and density according to the following equation:

$$D = \frac{6}{S_{BET} \times d} \qquad (2)$$

Electron microscopy (SEM) was used for morphological observations (Philips XL30, The Netherlands). The microstructure of sintered materials was revealed on mirror polished surfaces by thermal etching for 8 min at 20 °C below the sintering temperature in a CO_2 atmosphere. Sintered density of materials was obtained from sample weighing using the Archimedean method in water. The densification ratio was calculated by dividing the measured density by the theoretical density of each material. The theoretical (or maximum) density was calculated from the crystallographic data[9,24] and the chemical composition of each material. As the composition of carbonated hydroxyapatites depended on the sintering atmosphere, accordingly this calculated theoretical density varied as indicated in Table 2.

3. Results and discussion

3.1. Powders synthesis and characterization

The XRD patterns of raw powders (Fig. 1) showed that all the compositions had an apatitic structure (PDF 9-432). However, the sample C2 contained calcite $CaCO_3$ (PDF 5-586) as a second phase. A previous study[24] based on a similar synthesis process identified the presence of calcite when the ratio $(C/P)_{reagents}$ was above 3/2, which agrees with our results. Fig. 2 gives the carbonate content (CO_3 wt%) of raw powders versus the initial molar ratio of reagents $(C/P)_{reagents}$. The carbonate content increased reproducibly with the $(C/P)_{reagents}$ up to a value of 7.5 wt% for the composition C2. But, for this last one the measured value resulted from the contribution of both carbonated apatite and calcite phases. The higher carbonate loading of single-phased powders, i.e., for composition C1, was 7.34 ± 0.25 wt%.

All the single-phased compositions of raw powders had the same specific surface area with a value of about 36 $m^2\,g^{-1}$. Pycnometry analyses gave density values for carbonated apatite powders and pure HA around 2.8 ± 0.1, the values decreasing slowly with increasing carbonate content (Table 3). These values were lower than the calculated values of maximum density (Table 2). This can be explained by the low crystallinity (due to the presence of lattice defects, see Eq. (3)) of the precipitated powders as shown on XRD patterns (Fig. 1). The more the pow-

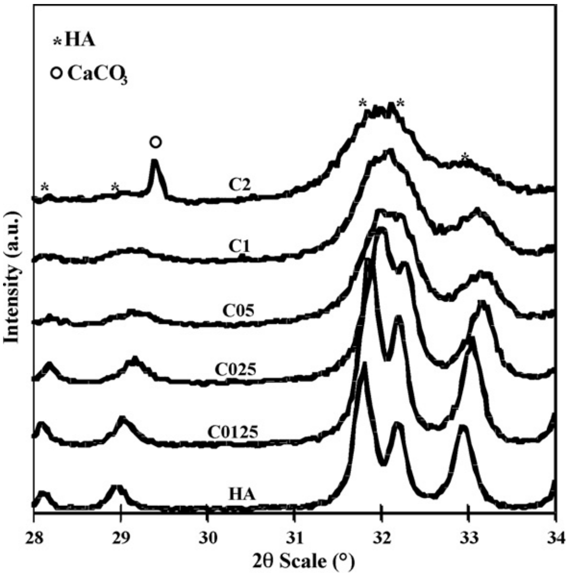

Fig. 1. XRD patterns of as synthesized powders.

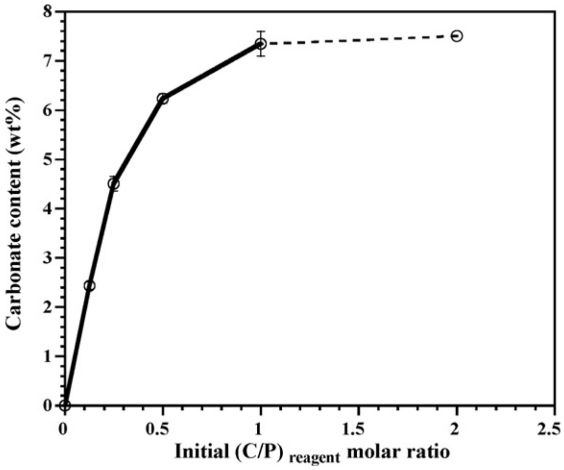

Fig. 2. Carbonate content (wt%) of powders vs. the initial $(C/P)_{reagent}$ molar ratio.

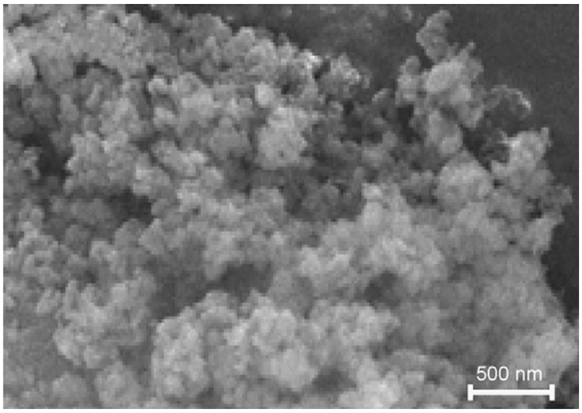

Fig. 3. Typical SEM image of raw powders (sample C05).

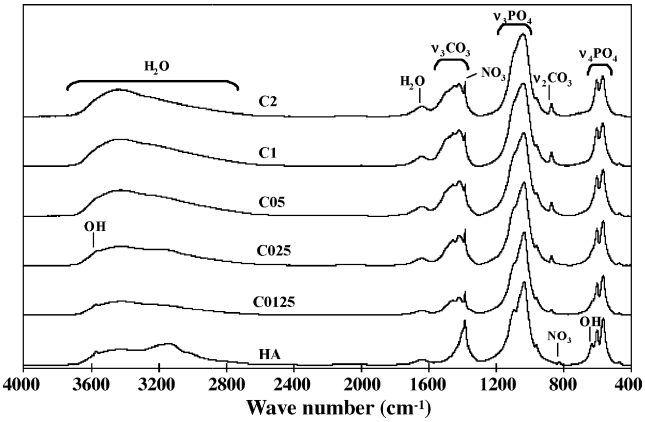

Fig. 4. FTIR spectra of as synthesized powders.

der is carbonated the more the diffraction peaks broaden. This phenomenon could originate from either a decrease of crystallite size or a decrease of crystallinity of powders.[25] Powders surface and density values allowed the calculation of an average grain size of approximately 60 nm for all the powders (Eq. (2), Table 3), which was confirmed by SEM images (Fig. 3). Thus, the decrease of density with increasing carbonate content is associated with a lower crystallinity of the powders.

The surface area and density of composition C2 (i.e., 50.6 $m^2 g^{-1}$ and 2.83, respectively) differ slightly from the others. This was due to the presence of calcite as a secondary phase in the powder. Because the aim of this work was to investigate pure carbonated apatites, the presence of any secondary minor phase was not suitable. So, composition C2 was not used in the sintering part of this study.

The FTIR spectra (Fig. 4) showed that all the compositions exhibited the characteristic bands of phosphate groups of the apatitic structure at about 550 and 600 cm^{-1} (ν_4), 960 cm^{-1} (ν_1), 1020–1120 cm^{-1} (ν_3). The bands at 630 and 3540 cm^{-1} were assigned to apatitic OH groups. The intensity of these last bands decreased as the carbonate content increased. The broad bands in the regions 1600–1700 and 3200–3600 cm^{-1} corresponded to adsorbed water. The band at 1380 cm^{-1} was attributed to residual nitrates resulting from synthesis precursors. It was particularly visible on the IR spectrum of HA powder that was not washed after synthesis. Hydrogenphosphate ions are sometimes present in synthetic carbonated apatites because they can easily substitute for phosphate ones in the apatite structure during the synthesis.[26] They are characterized by a vibration band at about 875 cm^{-1} that was never detected on the spectra. Their absence in the powders is all the more important as they lead to substantial modifications of the chemical composition and thermal behaviour of compounds.[27] Two regions of the spectra are characteristic of carbonate vibrations in apatites:

(i) 850–890 cm^{-1} associated with ν_2 vibrations of carbonate groups,
(ii) 1400–1650 cm^{-1} associated with ν_3 vibrations of carbonate groups.

They are detailed on zooms Fig. 5a and b. The bands were assigned to carbonate vibrations in A or B site of the apatite in agreement with the literature data summarized in Table 4. Carbonate groups appeared located in B sites. But, from these

Table 3
Characteristics of as synthesized powders

Sample	Surface area ($m^2 g^{-1}$)	Density	Average grain size (nm)	Average carbonate content (wt%)	Chemical formula
HA	34.2	2.91	60	0	$Ca_{10}(PO_4)_6(OH)_2$
C0125	36.3	2.83	58	2.43 ± 0.08	$Ca_{9.60}(PO_4)_{5.60}(CO_3)_{0.40}(OH)_{1.60}$
C025	35.9	2.82	59	4.50 ± 0.15	$Ca_{9.30}(PO_4)_{5.30}(CO_3)_{0.70}(OH)_{1.30}$
C05	36	2.80	60	6.23 ± 0.10	$Ca_{9.05}(PO_4)_{5.05}(CO_3)_{0.95}(OH)_{1.05}$
C1	36.9	2.76	59	7.34 ± 0.25	$Ca_{8.90}(PO_4)_{4.90}(CO_3)_{1.10}(OH)_{0.90}$
C2	50.6	2.83	n.d.	7.50	Carbonated apatite + $CaCO_3$

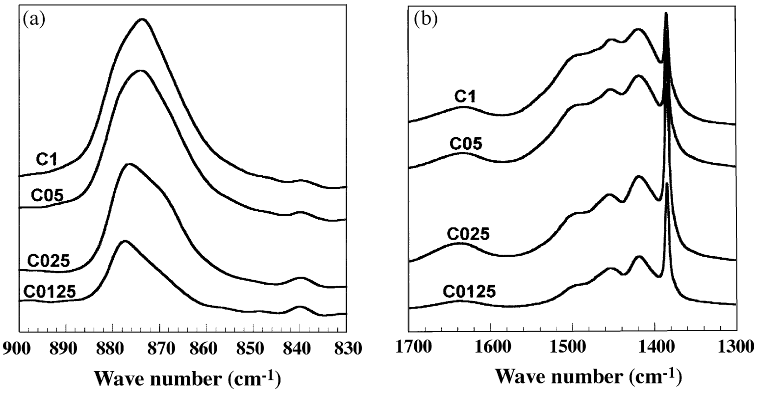

Fig. 5. FTIR spectra of carbonate vibrations in calcium phosphate apatites: (a) ν_2 domain; (b) ν_3 domain.

Table 4
Infrared vibration bands of carbonate groups in calcium phosphate apatites

Type	ν_2	ν_3	Reference
A-type	880	1545, 1450	26
A-type	878	1540, 1500, 1465	28
B-type	873	1465, 1412	26
(CO_3) B-type	871	1470, 1420	28
(CO_3,OH) B-type	871	1460, 1420	28
$CO_3{}^{2-}$ absorbed	866		23
A or B-type		1452, 1470, 1500, 1545, 1568	23

IR spectra, the presence of carbonate in A sites could not be totally excluded, so that complementary Raman microspectrometry was performed. This technique allows the quantification of carbonate content in A and B sites according to a procedure described by Penel et al.[29] It confirmed that all the powders were B-type carbonated apatites.

Finally, according to the whole results, the following chemical formula could be given for the synthesized powders, which corresponds to pure B-type carbonated hydroxyapatites:

$$\mathrm{Ca}_{10-x}(V''_{\mathrm{Ca}})_x(\mathrm{PO}_4)_{6-x}(\mathrm{CO}_3)_x(\mathrm{OH})_{2-x}(V^{\mathrm{o}}_{\mathrm{OH}})_x \qquad (3)$$

where V''_{Ca} and $V^{\mathrm{o}}_{\mathrm{OH}}$ represent, respectively the calcium and hydroxide vacancies.

The chemical composition of each powder was determined from its average carbonate content (Table 3) an Eq. (3). The resulting formulae are summarized in Table 3.

3.2. Sintering and characterization of ceramics

3.2.1. Linear shrinkage

The influence of the initial content of carbonate in B sites on the sintering behaviour was investigated by dilatometry. In argon atmosphere, linear shrinkage (Fig. 6a) and derivative plots (Fig. 6b) indicated a classical behaviour for pure HA: the shrinkage began at about 800 °C and its rate was maximum at 1080 °C. For carbonated apatites, the beginning of shrinkage shifted to slightly lower temperatures at about 750–780 °C. Then, it seemed to proceed in two steps with a marked slowing in the 900–950 °C temperature range (Fig. 6b). The first step, with an apparent maximum at about 900 °C was more precisely an acceleration of shrinkage due to the decomposition of carbonated apatites. We have demonstrated in a previous paper that this thermal decomposition began from about 600 °C in inert atmosphere and that a CO_2 gas atmosphere made it possible to stabilize the carbonated structure up to about 900 °C.[30] The decomposition of carbonated apatites produces CO_2 evolution and formation of HA $\mathrm{Ca}_{10}(\mathrm{PO}_4)_6(\mathrm{OH})_2$ and lime CaO. These

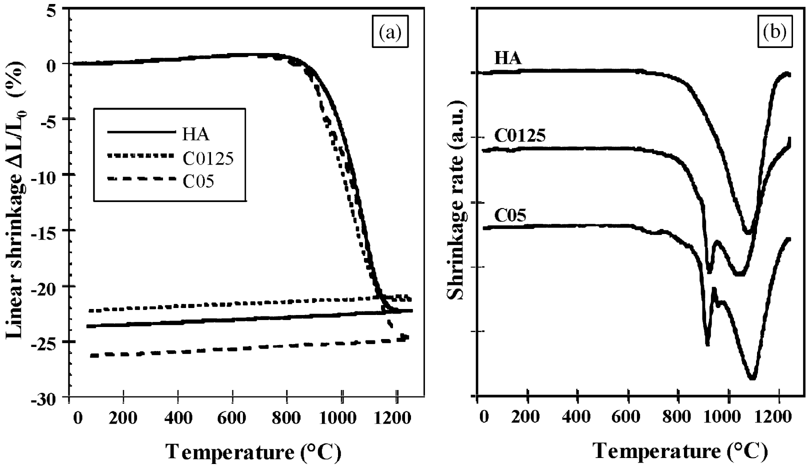

Fig. 6. TMA. (a) Linear shrinkage of apatite samples heated in argon atmosphere vs. the temperature. (b) Derivative plots of linear shrinkage.

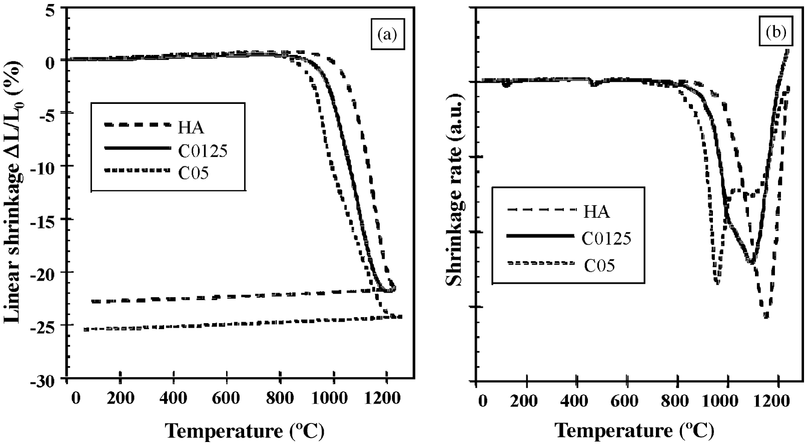

Fig. 7. TMA. (a) Linear shrinkage of apatite samples heated in CO_2 atmosphere vs. the temperature. (b) Derivative plots of linear shrinkage.

phenomena are accompanied, respectively by a mass decrease of the sample and by a marked increment of its bulk density, the values for carbonated apatites being smaller than those of pure HA and CaO (see Table 2, density of CaO: 3.35). As a result, the sample volume contracts, which explains the high shrinkage rate. Then, above 950 °C the material is made of a mixture of HA containing CaO as a minor phase and the behaviour became again similar to that of HA.

In CO_2 atmosphere (Fig. 7a and b), as in argon, the sintering began at a temperature that decreased noticeably when the initial carbonate content increased. This phenomenon was already observed.[15] It could be explained by the increase of the concentration of calcium and hydroxide vacancies in the apatite structure when carbonate content in B-site increased (Eq. (3)). Indeed, it is known that the solid state diffusion (volume, grain boundaries or superficial diffusion mechanism) is influenced by the nature and concentration of punctual defects in the solid. The creation or the presence of vacancies of the limiting species always activates the sintering. Thus, the simultaneous increase of cationic and anionic vacancies in B-site carbonated hydroxyapatites should enhance the sintering. The same hypothesis can be made for the temperature shift registered in argon atmosphere. The main difference or behaviour between the two atmospheres came from the stabilization of carbonate apatite structure up to higher temperatures. This effect is shown in Fig. 7b. The apparent acceleration that resulted from the decomposition of the carbonated structure shifted towards higher temperature and this shift was all the more important if the initial carbonate content of the apatite was low: 950 °C and around 1000 °C for compositions C05 and C0125, respectively, against 900 °C in argon (Fig. 6b). This behaviour agrees with previous studies that showed that the thermal stability of carbonated apatites depends on their carbonate content, the decomposition temperature decreasing with the increase of carbonation.[17,31,32]

In other respects, it can be noted that the highest shrinkage rate for HA occurred at about 1150 °C in CO_2 atmosphere, i.e., at 70 °C higher than in argon atmosphere (Fig. 8). This indicated that though pure HA is stable in this temperature range, the atmosphere influenced its sintering behaviour. Only the composition of A sites of the HA is modified by the CO_2 atmosphere during heating according to the carbonation reaction Eq. (1). In order to confirm this influence a sample of pure A-type carbonated apatite containing 4.2 wt% of carbonate in A site (obtain after heating a HA powder for 24 h at 900 °C in dry CO_2 atmosphere) was also heated in CO_2 gas. For this sample, the maximum shrinkage rate was registered at about 1200 °C (Fig. 8). From these results it can be stated that the presence of carbonate in A sites of the apatites or the carbonation of A site that occurs during the thermal treatment of HA or B-type carbonated apatites in CO_2 gas atmosphere was detrimental to the sintering of calcium phosphate apatites.

3.2.2. Influence of water vapour

Independently of the decomposition of B-type carbonated apatites and depending on the atmosphere, carbonation–hydroxylation could take place in the A sites

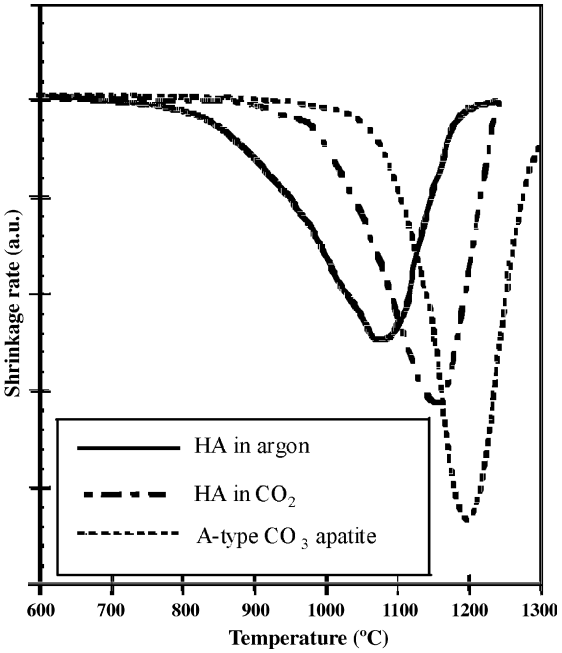

Fig. 8. TMA. Derivative plots of linear shrinkage of HA and A-type carbonated apatite vs. the temperature in argon or CO_2 atmosphere.

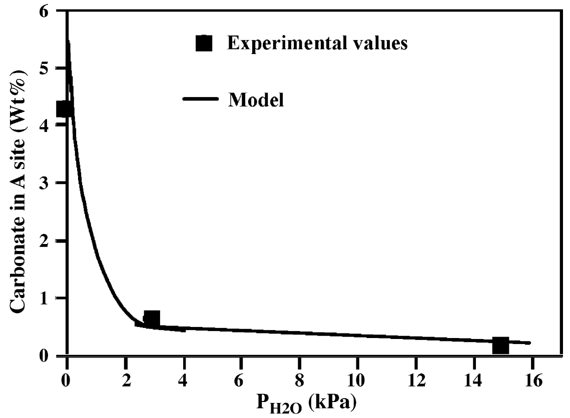

Fig. 9. Predicted and experimental values of carbonate content in A sites vs. the partial pressure P_{H_2O} for HA samples heated under $P_{CO_2} = 50$ kPa at $T = 870$ °C.

of the apatite during heating according to the reversible reaction Eq. (1). This system is governed by the partial pressure of H_2O (P_{H_2O}), the partial pressure of CO_2 (P_{CO_2}) and the temperature. Quasi-chemical equilibria and structural elements were used to establish a mathematical representation of this system, allowing prediction of the composition of A sites at the thermodynamic equilibrium versus P_{H_2O}, P_{CO_2} and T.[31] Fig. 9 gives an example of the predicted carbonate content in A sites of the apatite at the equilibrium versus P_{H_2O}, for fixed values of P_{CO_2} (50 kPa) and temperature (870 °C). The model was experimentally verified with several HA samples heated in the same conditions (some values of interest are given in Fig. 9). As expected, the A site carbonation could be controlled by the partial pressure of water vapour. More, the values showed that carbonation can be drastically limited in the presence of a very low pressure of water vapour. Indeed, a partial pressure of only 3 kPa of water vapour in the atmosphere was enough to reduce the carbonate content in A sites at the equilibrium from 5.5 wt% in dry CO_2 atmosphere down to 0.5 wt% (values at 870 °C and 50 kPa of CO_2).

Finally, the introduction of a partial pressure of water vapour P_{H_2O} in the CO_2 atmosphere during heating limits the carbonation of A sites of apatites and indirectly enhances the sintering of carbonated apatites. This noteworthy result was used in the sintering study.

3.2.3. Sintering experiments

In order to prevent the decomposition of B-type carbonated apatites, all the sintering tests were performed with a constant partial pressure of CO_2 gas $P_{CO_2} = 50$ kPa. The influence of water vapour on the sintering was verified using several partial pressures. The sintering was actually enhanced in the presence of water vapour. Such a tendency was already observed by Barralet et al.[16] on sodium containing carbonated apatites, but was not explained yet. Both the time at constant temperature and the temperature at constant time required to reach a given densification ratio decreased with increasing partial pressure of water in the sintering atmosphere. An example is given in Table 5 for composition C0125. A densification ratio of 70% could be reached at 900 °C for only 15 min while 1 h was necessary in dry CO_2–Ar atmosphere. Similarly, it was possible to nearly fully densify (up to 97% of the calculated value d_{th}) this same composition at 900 °C for 1 h with 3 kPa of water vapour in the sintering atmosphere, while 950 °C was necessary to reach a densification ratio of 95% in dry atmosphere.

Table 5
Influence of the partial pressure of water vapour on the time (at 900 °C) or temperature (for 60 min) of sintering ($P_{CO_2} = 50$ kPa) for sample C0125

P_{H_2O} (kPa)	Densification ratio (% d_{th})	Temperature (°C)	Time (min)
0	70	900	60
3	70	900	30
15	70	900	15
0	95	950	60
3	97	900	60

Thus, water vapour appeared greatly helpful to sinter B-type carbonated apatites without decomposition because it allowed to decrease noticeably the temperature, which is the crucial parameter for the thermal stability of such materials. But, a drawback can be encountered when a partial pressure of water vapour is used because it seemed to catalyze the decomposition of B-type carbonated apatites. As a result, the most carbonated compositions treated in wet CO_2 atmosphere were partially decomposed after sintering. But, though B-type apatites highly loaded in carbonate ions decomposed at a lower temperature than the more lightly carbonate loaded materials, their sintering occurred also at a lower temperature. For such compositions water vapour was not necessary to obtain nearly fully dense materials made of pure carbonated apatite. It could also be noticed that the presence of water vapour in the sintering atmosphere induced a more important grain growth than the sintering in a dry atmosphere. This result can relate to the catalytic effect of water vapour on superficial diffusion that induces grain coalescence during the heating of HA materials.[33]

Finally, depending on the initial carbonate content of samples, a compromise can be reached allowing the production of single phased and dense materials. By adapting the sintering parameters, i.e., temperature, time and atmosphere to each composition, all the carbonated apatites could be densified up to 97–98% of the theoretical density without decomposition. Examples of sintering parameters and corresponding characteristics of ceramics are summarized in Table 6. Using these conditions, the microstructure was homogeneous and similar whatever the composition might be. Fig. 10 gives a typical micrograph of one of them. It was characterized by a fine grain size ranging from 100 to 500 nm. The microstructural design of sintered parts is also an important parameter that must be controlled, too. Indeed,

Table 6
Examples of sintering parameters to produce dense single phased carbonated apatites

Sample	T (°C)	P_{H_2O} (kPa)	Time (min)	Densification ratio (%)
C0125	900	3	60	97
C025	900	0	30	98
C05	875	0	60	98

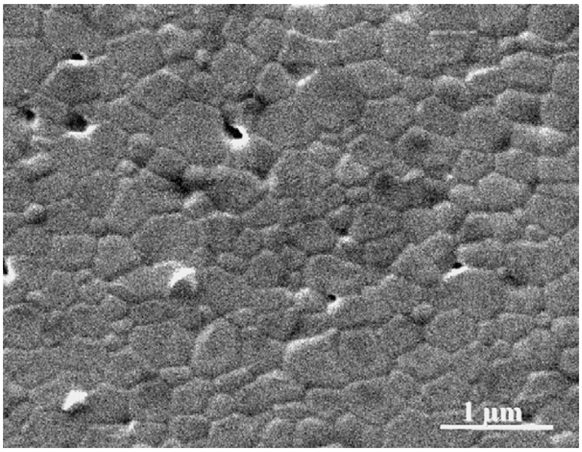

Fig. 10. Typical SEM micrograph of a sintered ceramic (composition C025).

grain size of ceramics should be ideally similar and as small as possible. These criteria are fundamentals for the mechanical properties and reliability of ceramics, which is important for further applications as bone graft substitutes.

4. Conclusion

The real composition but also the microstructure of ceramic surface may influence greatly the biological behaviour of calcium phosphate based apatites. Very recent papers have pointed out the effect of micropores on osteoinductive properties[34,35] or surface composition that, due to material processing, may differ from the bulk composition.[36] As numerous material parameters can influence the biological behaviour, the control of the processing parameters that govern the final properties of the material as well as the use of precise characterization methods are of prime importance for a good understanding of its behaviour in vitro or in vivo. In this paper, we have demonstrated the influence of CO_2 gas and water vapour on the sintering of carbonated apatites, more particularly in association with the role of the A-site composition. Processing parameters must be adjusted to each composition so that dense ceramics of sodium-free mixed A/B-type carbonated hydroxyapatite with controlled composition and a fine grain microstructure could be reproducibly produced.

The chemical composition of ceramics was that of a pure mixed A/B-type carbonated hydroxyapatite which could be described with the following formula:

$$\mathrm{Ca}_{10-x}(\mathrm{PO}_4)_{6-x}(\mathrm{CO}_3)_x(\mathrm{OH})_{2-x-2y}(\mathrm{CO}_3)_y$$

$$\text{with } 0 \le x \le 2 \text{ and } 0 \le y \le x/2 \tag{4}$$

where x and y correspond to the B-type and A-type carbonate contents, respectively. Without decomposition during sintering, the composition of the final ceramic could be entirely controlled:

- x was equal to the initial carbonate content of the powder. It was reproducibly controlled from 0 to 1.1 during the powder synthesis process.
- y was controlled by the sintering parameters from 0 to 0.2 (depending on the values of T, P_{H_2O}, P_{CO_2}) according to the equilibria of A sites Eq. (1).

The production of a series of dense or porous ceramic parts is now in progress for further biological evaluation of the amount and location sites of carbonate ions on the biological behaviour of these apatites.

Acknowledgements

The authors would like to thank Dr. Gérard Leroy, from the "Laboratoire de Biomatériaux" (Faculty of Dental Surgery, University of Lille) for Raman microspectrometry experiments. A part of this study was financially supported by the French program "Matériaux du Massif Central".

References

1. Groot, K. D., Ceramics of calcium phosphate: preparation and properties. In *Bioceramics of Calcium Phosphate*, ed. K. D. Groot. CRC Press, Boca Raton, FL, USA, 1983, pp. 99–114.
2. Jarcho, M., Calcium phosphate ceramics as hard tissue prosthetics. *Clin. Orthop. Rel. Res.*, 1981, **157**, 259–278.
3. Hench, L. L., Bioceramics: from concept to clinic. *J. Am. Ceram. Soc.*, 1991, **74**, 1487–1510.
4. Heise, U., Osborn, J. F. and Duwe, F., Hydroxyapatite ceramic as a bone substitute. *Int. Orthop.*, 1990, **14**, 329–338.
5. LeGeros, R. Z., Crystallography studies of the carbonate substitution in the apatite structure. Thesis. University of New York, 1967.
6. Legros, R., Balmain, N. and Bonel, G., Structure and composition of the mineral phase of periosteal bone. *J. Chem. Res.*, 1986, **S**, 8–9.
7. Elliott, J. C., Holcomb, D. W. and Young, R. A., Infrared determination of the degree of the substitution of hydroxyl by carbonate ions in human dental enamel. *Calcif. Tissue Int.*, 1985, **37**, 372–375.
8. Tadic, D., Peters, F. and Epple, M., Continuous synthesis of amorphous apatites. *Biomaterials*, 2002, **23**, 2553–2559.
9. Bonel, G., Contribution à l'étude de la carbonation des apatites -1- Synthèse et étude des propriétés physico-chimiques des apatites carbonatées du type A. *Annales de Chimie Fr.*, 1972, **7**, 65–88.
10. Vignoles, M., Bonel, G., Holcomb, D. W. and Young, R. A., Influence of preparation conditions on the composition of type B carbonated hydroxyapatite and on the localization of the carbonate ions. *Calcif. Tissue Int.*, 1988, **43**, 33–40.
11. Vignoles, C., Contribution à l'étude de l'influence des ions alcalins sur la carbonation dans les sites B des apatites phosphocalciques. Thesis. University of Toulouse, France, 1973.
12. Doi, Y., Shibutani, T., Moriwaki, Y., Kajimoto, T. and Iwayama, Y., Sintered carbonate apatites as bioresorbable bone substitute. *J. Biomed. Mater. Res.*, 1998, **39**, 603–610.
13. Barralet, J., Akao, M., Aoki, H. and Aoki, H., Dissolution of dense carbonate apatite subcutaneously implanted in wistar rats. *J. Biomed. Mater. Res.*, 2000, **49**, 176–182.
14. Hazegawa, M., Doi, Y. and Uchida, A., Cell-mediated bioresorption of sintered carbonate apatite in rabbits. *J. Bone Joint Surg.*, 2003, **85(B)**, 142–147.
15. Doi, Y., Koda, T., Wakamatsu, N., Goto, T., Kamemizu, H., Moriwaki, Y. *et al.*, Influence of carbonate on sintering of apatites. *J. Dental Res.*, 1993, **9**, 1279–1284.
16. Barralet, J. E., Best, S. M. and Bonfield, W., Effect of sintering parameters on the density and microstructure of carbonate hydroxyapatite. *J. Mater. Sci.: Mater. Med.*, 2000, **11**, 719–724.
17. Barralet, J. E., Knowles, J. C., Best, S. M. and Bonfield, W., Thermal decomposition of synthesized carbonate hydroxyapatite. *J. Mater. Sci.: Mater. Med.*, 2002, **13**, 529–533.

18. Ishikawa, K., Ishikawa, Y. and Kuwayama, N., Preparation of carbonate-bearing HAP and their sintering properties. *Chem. Express*, 1991, **6**, 463–466.
19. Tonsuaadu, K., Peld, M. and Leskela, T., A thermoanalytical study of synthetic carbonate containing apatites. *Thermochim. Acta*, 1995, **256**, 55–65.
20. Landi, E., Tampieri, A. and Celotti, G., Influence of synthesis and sintering parameters on the characteristics of carbonate apatite. *Biomaterials*, 2004, **25**, 1763–1770.
21. Bonel, G., Contribution à l'étude de la carbonation des apatites -3- Synthèse et étude des propriétés physico-chimiques d'apatites carbonatée dans deux types de sites. Evolution des spectres IR en fonction de la composition des apatites. *Annales Chimie Fr.*, 1972, **7**, 140–144.
22. Gibson, I. R. and Bonfield, W., Novel synthesis and characterization of an AB-type carbonate-substituted hydroxyapatite. *J. Biomed. Mater. Res.*, 2001, **59**, 697–708.
23. Rey, C., Collins, B., Goehl, T., Dickson, I. R. and Glimcher, M. J., The carbonate environment in bone mineral: a resolution enhanced Fourier transform infrared spectroscopy study. *Calcif. Tissue Int.*, 1989, **45**, 157–164.
24. Labarthe, J. C., Bonel, G. and Montel, G., Sur la structure et les propriétés des apatites carbonatées de type B phospho-calciques. *Annales Chimie Fr.*, 1973, **8**, 289–301.
25. Baig, A. A., Fox, J. L., Young, R. A. and Wang, Z., Relationships among carbonated apatite solubility, crystallite size, and microstrain parameters. *Calcif. Tissue Int.*, 1999, **64**, 437–449.
26. Elliott, J. C., *Structure and Chemistry of the Apatites and Other Calcium Orthophosphates*. Elsevier Science B.V., Amsterdam, 1994.
27. Raynaud, S., Champion, E., Bernache-Assollant, D. and Thomas, P., Calcium phosphate apatites with variable Ca/P atomic ratio I. Synthesis, characterization and thermal stability of powders. *Biomaterials*, 2002, **23**, 1065–1072.
28. Vignoles, M., Contribution à l'étude des apatites carbonates de type B. Thesis. Institut National Polytechnique de Toulouse, 1984.
29. Penel, G., Leroy, G., Rey, C. and Lemaitre, J., Qualitative and quantitative investigation on calcium phosphate of biological interest by raman microspectrometry. *Rec. Res. Dev. Appl. Spectrosc.*, 1999, **2**, 137–146.
30. Lafon, J. P., Champion, E., Bernache-Assollant, D., Gibert, R. and Danna, A. M., Thermal decomposition of carbonated calcium phosphate apatites. *J. Therm. Anal. Calorim.*, 2003, **72**, 1127–1134.
31. Lafon, J. P., Synthèse, stabilité thermique et frittage d'hydroxyapatites carbonatées. Thesis. University of Limoges, 2004.
32. Khattech, I. and Jemal, M., Décomposition thermique de fluorapatites carbonatées de type B "inverses". *Thermochim. Acta*, 1987, **118**, 267–275.
33. Bernache-Assollant, D., Ababou, A., Champion, E. and Heughebaert, M., Sintering of calcium phosphate $Ca_{10}(PO_4)_6(OH)_2$ I. Calcination and particle growth. *J. Eur. Ceram. Soc.*, 2003, **23**, 229–241.
34. Habibovic, P., Yuan, H., van der Valk, C. M., Meijer, G., van der Blitterswijk, C. A. and de Groot, K., 3D microenvironment as essential element for osteoinduction by biomaterials. *Biomaterials*, 2005, **26**, 3565–3575.
35. Le Nihouannen, D., Daculsi, G., Saffarzadeh, A., Gauthier, O., Deplace, S., Pilet, P. *et al.*, Ectopic bone formation by microporous calcium phosphate ceramic particles in sheep muscles. *Bone*, 2005, **36**, 1086–1093.
36. Pellenc, D., Giraudier, S., Champion, E., Anselme, K., Larreta-Garde, V. and Gallet, O., Removal of surface by-products from sintered hydroxyapatite: effect of a chelation treatment on fibronectin adsorption and cell adhesion. *J. Biomed. Mater. Res. B: Appl. Mater.*, 2006, **76B**, 136–142.